Tanzania Journal of Science 44(4): 51-58, 2018 ISSN 0856-1761, e-ISSN 2507-7961

Compositional and Thickness Effects on the Optical Properties of Zinc–Doped Selenium–Antimony Thin Films

Austine A Mulama[1, 2*], Julius M Mwabora[1], Andrew O Oduor[2] and Cosmas M Muiva[3]

[1]*Department of Physics, University of Nairobi, 30197-00100, Nairobi Kenya*

[2]*Department of Physics and Materials Science, Maseno University, 333-40105, Maseno Kenya*

[3]*Department of Physics, Botswana International University of Science and Technology, 00741, Botswana*

**Corresponding author e-mail: mulamaustine@gmail.com*

Abstract

Chalcogenide system of antimony (Sb)-selenium (Se)-zinc (Zn) system is a promising semiconductor for phase change memory devices due to its thermal stability and low power consumption. The study investigated the effect of film thickness and zinc content on the optical properties of thermally evaporated $Sb_{10}Se_{90-x}Zn_x$ (x = 0, 5, 10 & 15 at. %) thin films. It was found that transmittance (T~ 85-40%) and optical band gap energy (E_{opt} ~ 1.60 eV – 1.22 eV) decreased but absorption coefficient (α~0.840–2.031 $\times 10^4$ cm^{-1}) increased with increase in zinc content. Furthermore, as the film thickness increased from 53 ± 5 nm to 286 ± 10 nm, transmittance decreased but band gap energy increased due to zinc defects and localized states in the $Sb_{10}Se_{90-x}Zn_x$ system.

Keywords: Selenium, phase change memory, localized states

Introduction

Amorphous selenium (a-Se) semiconductor is an attractive chalcogenide material. However, pure a-Se experiences unusual ageing behaviour, unexpected thermal instabilities and deformed chain conformations (Nasir et al. 2011, Abdel-Rahim et al. 2015). This can be eliminated through doping with other elements like tellurium (Te), copper (Cu), arsenic (As), zinc (Zn), bismuth (Bi) and antimony (Sb) (Muiva et al. 2012, Sharma et al. 2013, Sharma et al. 2014, Mulama et al. 2015). Structural dynamics in these types of glasses is important in understanding their transport mechanisms. Doping Se-based chalcogenide systems with Zn leads to improved material strength by cross-linking Se-glassy matrix (Abdel-Rahim et al. 2015). The elements such as Sb cause the structural disorders which may tune the optical and electrical properties of a ternary Sb-Se-Zn material, useful in phase change memory technology (Nasir and Zulfequar 2012, Nidhi et al. 2013). Adding Zn to the Sb-Se binary system may transform it into a nonstoichiometric material and this greatly increases the compositional range over which rapid crystallization can be achieved.

Despite several studies done on glasses of Sb-Se system, its properties on a micro-scale with respect to effects of the preparation conditions on the optical properties have not been fully investigated (Nidhi et al. 2013, Mulama et al. 2014, Kolobov et al. 2015). A comprehensive investigation of the effect of processing pathways such as composition, film thickness, and substrate characteristics on the optical and structural properties of Sb-Se-Zn thin films is lacking. The aim of this study was to find out the effects of Zn impurities and film thickness on the optimization of optical characteristics of Se-Sb systems for reliability and scalability. These findings will permit identifying the best optimized properties of Sb-Se-Zn thin films.

Materials and Methods

The bulk glass samples of $Sb_{10}Se_{90-x}Zn_x$ (x = 0, 5, 10 and 15 at. %) were synthesized using melt quench technique. Raw materials Zn, Sb and Se (99.999% 5 N pure) were used. Quartz glass ampoules (outer diameter of 1.0 cm and inner diameter of 0.8 cm) were cleaned in acetone, methanol and followed by rinsing in deionised water. The individual elements were weighed according to their atomic weight percentages followed by sealing of the mixtures in evacuated quartz ampoules. The sealed quartz ampoules were transferred to a rotary electric furnace and heated gradually at a heating rate of 4 °C per minute to prevent explosion, oxidation and hydrolysis in the sealed ampoules (Mulama et al. 2015). For the case of Sb-Se-Zn under investigation, the temperature of the furnace was raised to 300 °C, 500 °C and 800 °C so that Se (T_m = 221 °C), Zn (T_m = 420 °C), Sb (T_m = 631 °C) diffused into the rest of the constituents (Nidhi et al. 2013). The ampoules were maintained at 800 °C with rocking for 24 hours to make the melt homogeneous. The quenching (at 800 °C) was done in ice-cooled water to ensure a continuous homogeneous mixture. The ampoules were broken to obtain the solid alloy that was crushed to fine powder with a pestle and mortar for thermal evaporation.

Measured thicknesses of the deposited films on a quartz crystal digital thickness monitor (Model DTM-101) were 53 ± 5 nm, 108 ± 6 nm, 210 ± 8 nm and 286 ± 10 nm. The substrate temperature was maintained at 50 °C. Thin films were kept in the deposition chamber for 24 hours to attain thermodynamic equilibrium. The amorphous nature of the deposited films was verified by X-Ray Diffraction machine (Phillips PW3710, UK). Transmittance and reflectance were measured on a SolidSpec.3700 DUV, spectrophotometer (SolidSpec.3700 DUV, Kyoto-Japan). The optical transmission spectra wavelength range was 200-2500 nm.

The refractive index was determined from Equation (1) (Swanepoel 1983).

$$n = \sqrt{N + \sqrt{\left(N^2 - n_s^2\right)}} \qquad (1)$$

Where

$$N = 2n_s\left(T_M - T_m\right)/T_M T_m + \left(n_s^2 + 1\right)/2\,;$$

T_M, T_m, are the maximum and minimum transmittance envelope functions, respectively, while n_s is the substrate refractive index. The expressions for real and imaginary parts of dielectric constant are given by

$$\varepsilon_1 = n^2 - k^2 \qquad (2)$$

$$\varepsilon_2 = 2nk \qquad (3)$$

where ε_1, ε_2 are the real and imaginary parts of the dielectric constant, k is the extinction coefficient (Goswami 2005, Ohring 2001).

The band gap energy was calculated from Equation (4) (Born and Wolf 1999);

$$\alpha h\nu = \delta\left(h\nu - E_{opt}\right)^2 \qquad (4)$$

where $\alpha = 4\pi k/\lambda$ is the absorption coefficient, λ is the wavelength, δ is a constant, $h\nu$ is the photon energy, and E_{opt} is the optical band gap energy.

Results and Discussion

Structural characterization

Figure 1 gives the X-ray diffraction patterns for 53 nm $Sb_{10}Se_{90-x}Zn_x$ (x = 0, 5, 10 & 15 at. %) thin films. No prominent peaks were observed, a signature of amorphous system (Nidhi et al. 2013, Mulama et al. 2014, Kolobov et al. 2015).

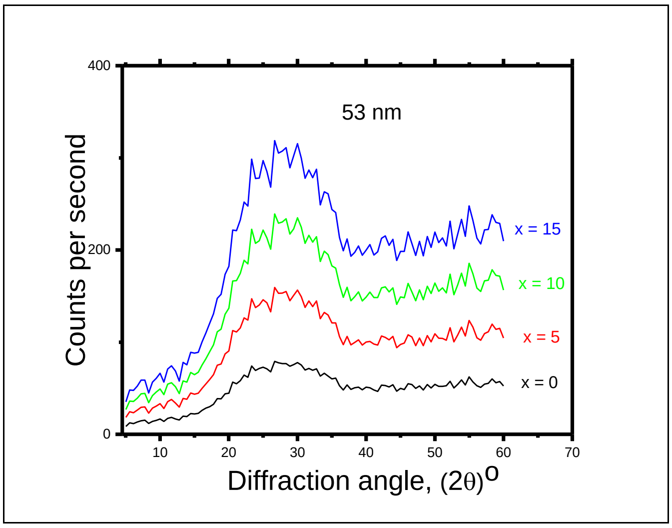

Figure 1: X-Ray Diffraction spectra of 53 nm $Sb_{10}Se_{90\text{-}x}Zn_x$ thin films.

Transmittance and reflectance

Transmittance against wavelength (nm) for the 53 nm $Sb_{10}Se_{90\text{-}x}Zn_x$ (x = 0, 5, 10 and 15 at. %) thin films has been plotted in Figure 2. Transmittance is almost zero (~0.04%) at very low wavelengths (λ ≤ 450 nm) due to light absorption in this region (Mulama et al. 2014, Abdel-Rahim et al. 2015). When zinc content increases from $x = 0\ \text{at.}\%$ to $x = 15\ \text{at.}\%$, the transmission of light in the deposited thin films reduces. This is mainly due to the effect of zinc introduced in the antimony-selenium system as impurity which absorbs part of the transmitted light. Increase in the film thickness leads to a decrease in transmittance in the deposited thin films. This is because thick films effectively increase the absorption path length in thin films (Mansour et al. 2010). This is an indication of increase in light absorption in the deposited thin films (Mulama et al. 2015). In addition, the interference fringes increased with increase in film thickness. This showed that the films were smooth and homogeneous.

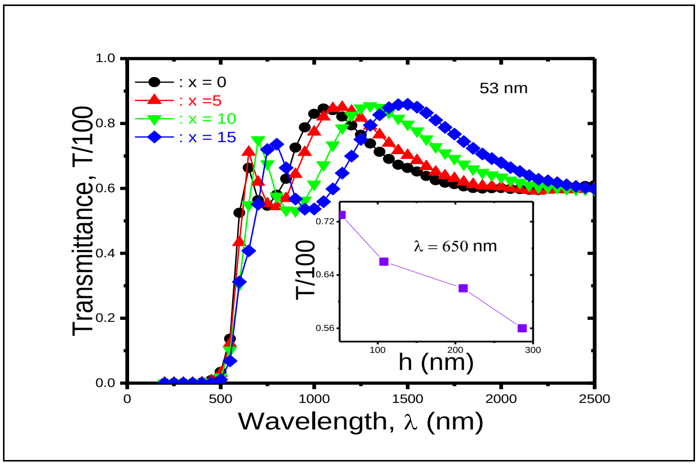

Figure 2: Transmittance against wavelength (nm) for a 53 nm $Sb_{10}Se_{90-x}Zn_x$ thin films (*Inset:* Transmittance against film thickness (nm) at λ = 650 nm).

Slight increase in reflectance with film thickness in the deposited thin films can be observed from Figure 3 as a result of decreased transmission of light in the deposited films with increase in film thickness. This may be an indication of less transparent films (Chauhan et al. 2013).

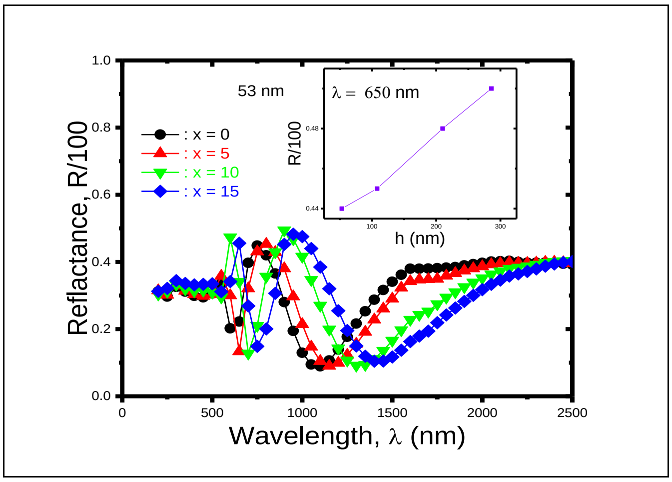

Figure 3: Reflectance against wavelength (nm) for a 53 nm $Sb_{10}Se_{90-x}Zn_x$ thin films (*Inset:* Reflectance against film thickness (nm) at λ = 650 nm).

Absorption coefficient

Remarkable increase in absorption coefficient in the $Sb_{10}Se_{90-x}Zn_x$ (x = 0, 5, 10 and 15 at. %) thin films was observed with increase in film thickness (Figure 4). This shows that an increase in film thickness leads to increase in the absorption path length in thin films (Aly et al. 2010, Mulama et al. 2014, Abdel-Rahim et al. 2015). In addition, the absorption coefficient was observed to increase with increase in zinc content, signaling an affinity to light for the $Sb_{10}Se_{90-x}Zn_x$ thin films. This has been observed in previous studies (Nasir et al. 2011, Nasir and Zulfequar 2012).

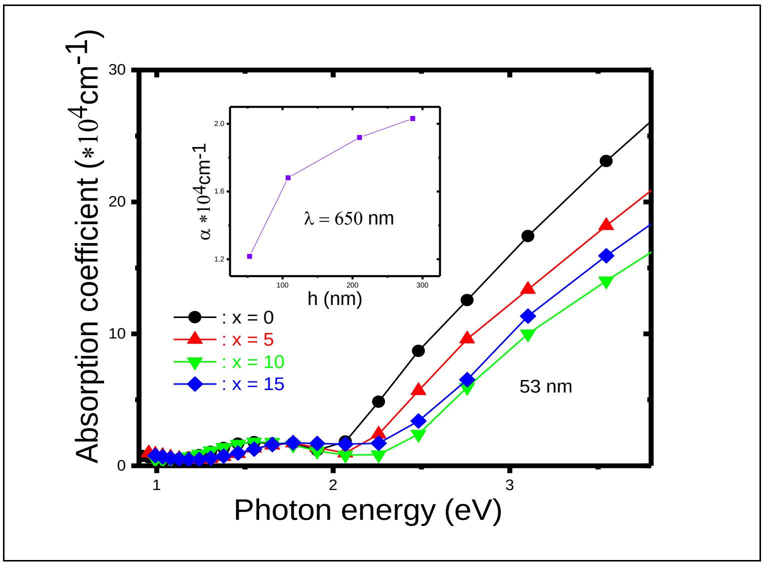

Figure 4: Absorption coefficient against photon energy (eV) for the 53 nm $Sb_{10}Se_{90-x}Zn_x$ thin films (*Inset:* Absorption coefficient against film thickness (nm) at λ = 650 nm).

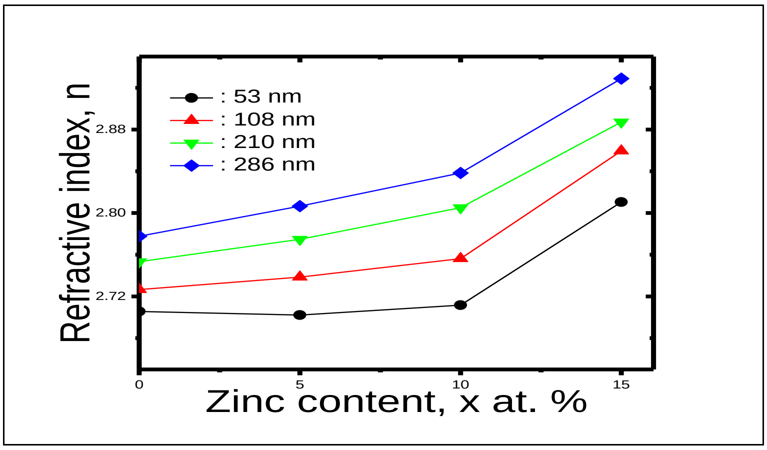

Figure 5: Refractive index against zinc concentration for $Sb_{10}Se_{90-x}Zn_x$ thin films at different film thickness, λ = 650 nm.

Refractive index

It was observed that the refractive index increased with increase in zinc concentration from $x = 0$ to $x = 15$ at. % (Figure 5) This may be due to the strong chemical disorder, zinc impurities and polarization in $Sb_{10}Se_{90-x}Zn_x$ system (Abdel-Rahim et al. 2015). The refractive index generally increased with increase in film thickness due to increased density of the deposited films as a result of zinc addition (Wee 2006).

Real and imaginary parts of dielectric constant

There is observed increase in the real part of dielectric constant with increase in zinc content in $Sb_{10}Se_{90-x}Zn_x$ (x = 0, 5, 10 and 15 at. %) thin films (Figure 6). In addition, the values of real part of the dielectric constant are greater than those for the imaginary part. This is an indication of increased absorption coefficient in the deposited thin films as already observed (Aly et al. 2010, Nasir and Zulfequar 2012).

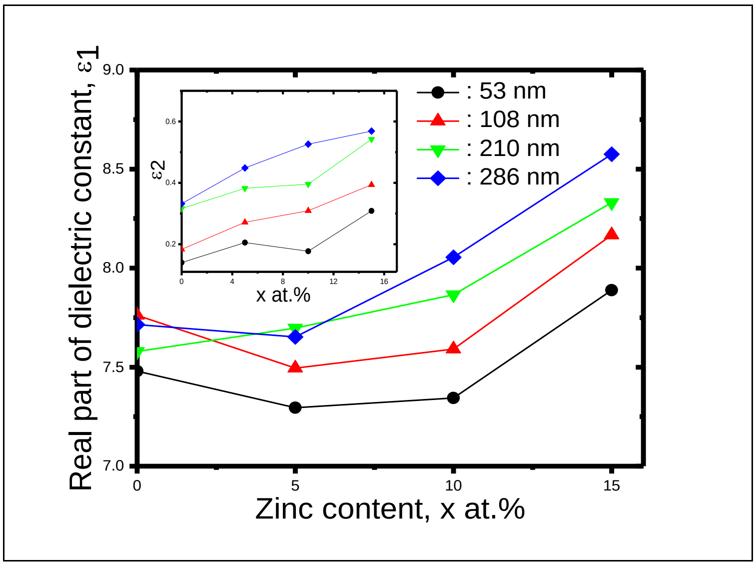

Figure 6: Real part of dielectric constant against zinc concentration for $Sb_{10}Se_{90-x}Zn_x$ thin films at different film thicknesses, λ = 650 nm (*Inset:* imaginary part of dielectric constant against zinc concentration).

Optical band gap energy

The optical energy band gap (Figure 7) was found by extrapolating the curves to the energy axis. The optical band gap energy was found to decrease with increase in zinc content. When zinc was added to antimony-selenium system, it introduced defect states in the amorphous antimony-selenium glass structure and this led to reduction in the optical band gap energy of the system (Nasir et al. 2011). Since the optical band gap energy depends on the strength of the kind of bonds that exist in the $Sb_{10}Se_{90-x}Zn_x$ system, the decrease in the optical band gap energy could be due to decrease in cohesive energy of the system (Aly et al. 2010, Mulama et al. 2014). Further, the optical band gap was observed to vary with film thickness. Similar trend has been observed by other authors (Mansour et al. 2010, Nidhi et al. 2013, Abdel-Rahim et al. 2015).

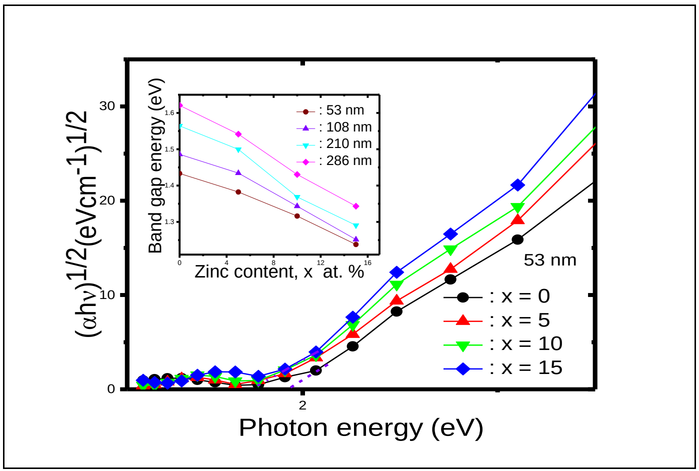

Figure 7: $(\alpha h\nu)^{1/2}(eV\,cm^{-1})^{1/2}$ against photon energy (eV) for 53 nm $Sb_{10}Se_{90-x}Zn_x$ thin films (*Inset:* Band gap energy (eV) against zinc content for different thickness (nm) at λ = 650 nm).

The band gap energy of the deposited $Sb_{10}Se_{90-x}Zn_x$ thin films varies with film thickness due to high density of dislocations resulting from zinc impurity in the system. It is noted that the optical band gap increased with increase in film thickness. This may be as a result of zinc defects and localized states in the $Sb_{10}Se_{90-x}Zn_x$ system (Mansour et al. 2010).

Conclusion

The deposited thin films of $Sb_{10}Se_{90-x}Zn_x$ were found to be amorphous as evidenced by absence of prominent peaks in the X-Ray diffraction patterns and the oscillatory nature of transmittance spectra. The optical band gap energy increased with increase in film thickness from 1.22 *eV* for 53 nm thin films to 1.60 *eV* for 286 nm thin films. The lowest optical band gap energy was observed at the highest zinc content i.e. $x = 15\ \text{at.}\,\%$ at 1.22 eV for the 53 nm. The high absorption coefficients observed in the range of 0.840 × 10^4 to 2.031 × 10^4 cm^{-1} the reduced transmittance (~40%) and the observed shift in the transmittance spectra towards higher wavelengths within the visible region with increase in film thickness in $Sb_{10}Se_{90-x}Zn_x$ thin films are indications of a photosensitive system.

Acknowledgements

The authors wish to acknowledge the financial support from the Government of Kenya under the National Research Fund (NRF) and the International Science Programme, Uppsala University through the Department of Physics, University of Nairobi for availing the research equipment.

References

Abdel-Rahim MA, Hafiz MM, Abdel-Latief AY, Abd-Elnaiem AM and Alwany, AEB 2015 A study of the non-isothermal crystallization kinetic of $Zn_{10}Se_{90}$ glass. *Appl. Phys. A* 119(3): 881-890.

Aly KA, Afify N and Aboushly AM 2010 Incorporation of Bi, Cd and Zn on the optical properties of $Ge_{20}Se_{80}$ thin films. *Phys. B: Condens. Matter.* 405(7): 1846-1851.

Born M and Wolf E 1999 Principles of Optics. 7th Ed., Cambridge University Press, London.

Chauhan R, Tripathi A, Srivastava AK and Srivastava KK 2013 Effect of swift heavy ion irradiation on optical and structural properties of amorphous Ge-As-Se thin films. *Chalc. Lett.* 10: 63-71.

Goswami A 2005 Thin Film Fundamentals. 5th Ed., New Age International Publishers, New Delhi.

Kolobov AV, Fons P, Krbal M, Tominaga J, Giussani A, Perumal K, Riechert H, Calarco R and Uruga T 2015 Local structure of epitaxial GeTe and $Ge_2Sb_2Te_5$ films grown on InAs and Si substrates with (100) and (111) orientations: An X-ray Absorption Near-Edge Structure Study. *J. Appl. Phys.* 117(125308): 1-7.

Mansour BA, Shaban H, Gad SA, El-Gendy YA and Salem AM 2010 Effect of film thickness, annealing and substrate temperature on the optical and electrical properties of $CuGa_{0.25}In_{0.75}Se_2$ amorphous thin films. *J. Ovon. Res.* 6: 13-22.

Muiva CM, Sathiaraj TS and Mwabora JM 2012 Chemical bond approach to optical properties of some flash evaporated $Se_{100-x}Sb_x$ chalcogenide alloys. *Eur. Phys. J. Appl. Phys.* 59: 1-7.

Mulama AA, Mwabora JM, Oduor AO and Muiva CM 2014 Optical properties and Raman studies of amorphous Se-Bi thin films. *The African Review of Physics* 9: 33-37.

Mulama AA, Mwabora JM, Oduor AO, Muiva CM, Amukayia BN and Mbete DA 2015 Role of bismuth and substrate temperature on the optical properties of some flash evaporated $Se_{100-x}Bi_x$ glassy system. *New J. Glass and Ceram.* 5(2): 16-24.

Nasir N and Zulfequar M 2012 DC conductivity and dielectric behavior of glassy $Se_{100-x}Zn_x$ alloy. *Open J. Inorganic Non-Metallic Materials* 2: 11-17.

Nasir M, Khan MAM, Husain M and Zulfequar M 2011 Thermal properties of $Se_{100-x}Zn_x$ glassy system. *Mater. Sci. Applicat.* 2(05): 289-292.

Nidhi AV, Modgil V and Rangra VS 2013 The effect of compositional variation on physical properties of $Te_9Se_{72}Ge_{19-X}Sb_x$ (X = 8, 9, 10, 11, 12) glassy material. *New J. Glass and Ceram.* 3(03): 91-98.

Ohring M 2001 The Material Science of Thin Films. Academic Press, London.

Sharma N, Sharda S, Sharma D, Sharma V, Barma PB, Katyal SC, Sharma P and Hazra SK 2013 Effect of substitutional doping on temperature dependence electrical parameters of amorphous Se-Te semiconductors. *Electron. Mater. Lett.* 9: 629-633.

Sharma N, Sharda S, Katyal SC, Sharma V and Sharma P 2014 Effect of Te on linear and non-linear optical properties of new quaternary Ge-Se-Sb-Te chalcogenide glasses. *Electron Mater. Lett.* 10: 101-106.

Singh AK 2013 A comparative study on optical properties of Se–Zn–In and Se–Zn–Te–In chalcogenide glasses. *Optik* 124(15): 2187-2190.

Swanepoel R 1983 Determination of the thickness and optical constants of amorphous silicon. *J. Phys. E: Sci. Instrum.* 16: 1214-1218.

Wee CT 2006 *Optical properties of amorphous selenium films*. MSc Thesis, University of Saskatchewan, Saskatoon, Canada.